

# Ionic Modulators of Electrophysiology and Re-entry Properties in Human Atria

C Sánchez<sup>1,2,3</sup>, B Rodríguez<sup>3</sup>, E Pueyo<sup>1,2,3</sup>

<sup>1</sup> Communications Technology Group, University of Zaragoza, Zaragoza, Spain

<sup>2</sup> Biomedical Research Networking Center in Bioengineering, Biomaterials and Nanomedicine (CIBER-BBN), Spain

<sup>3</sup> Computational Biology Group, Oxford University Computing Laboratory, Oxford, UK

## Abstract

*Current drugs used to treat atrial fibrillation (AF) often target tissue excitability (sodium channels) and refractoriness (hERG channels), but their efficacy is still modest. This study focuses on investigating new approaches to manage AF by conducting a systematic computer simulation study. The Maleckar action potential (AP) model was used to simulate human atrial cellular and tissue electrophysiology in control and AF-related electrically remodeled (AFER) conditions. Steady-state cellular AP duration (APD) and resting potential ( $V_{rest}$ ), as well as tissue properties, such as refractory period (ERP), conduction velocity (CV) and reentrant dominant frequency (DF) were quantified for default conditions and following changes in model parameters. Results are compared to experimental data from the literature for validation. Results show the fundamental role of the  $Na^+/K^+$  pump in electrophysiology and rotor dynamics in human atria through modulation of APD and ERP.  $I_{K1}$  controls re-entrant DF through modulation of AP, ERP and CV. Furthermore, the fast  $Na^+$  current ( $I_{Na}$ ) is key in determining DF through modulation of CV. The mechanisms underlying human atrial electrophysiological properties were qualitatively similar in control and AFER, although changes in ionic currents generally had smaller effects in AFER.*

## 1. Introduction

Atrial fibrillation (AF) is the most commonly diagnosed cardiac arrhythmia, with a 0.4-1% incidence in the overall population and over 8% incidence in patients over 80 years old. AF is an atrial arrhythmia considered to be sustained by both rapid ectopic activity and re-entrant circuits, whose establishment and stability are favoured by short refractory periods, slow conduction and long circuit pathways. AF-related electrical remodeling (AFER) following persistent AF causes alterations in those electrophysiological properties, which facilitate re-entrant activity and AF.

The aim of this study is to provide a systematic charac-

terization of the importance of ionic currents in modulating electrophysiology and rotor dynamics in human atria before and after AFER. A recently developed action potential (AP) cell model [1] is used, from which fiber and tissue models are built. Computational simulations are performed, which are validated using experimental data from the literature.

## 2. Methods

### 2.1. Cell model and simulations

The human AP model developed by Maleckar *et al.* [1] is used to investigate the impact of changes in ionic currents in modulating electrophysiological properties and rotor dynamics before (control) and after AFER. AFER is simulated by altering ion channel conductances ( $G_i$ ) as described in previous studies [2]: 70%  $G_{CaL}$  reduction; 50%  $G_{to}$  reduction; 50%  $G_{Kur}$  reduction; and 100%  $G_{K1}$  increment. Simulated human atrial cells are stimulated using 2-ms duration and twice diastolic threshold current pulses. AP duration (APD) at 90% repolarization and resting potential ( $V_{rest}$ ) are obtained after 20 min stimulation at a cycle length (CL) of 1000 ms.

Single alterations in the ionic conductances of the model between -100% and +100% from their default values are simulated, though  $\pm 30\%$  alterations are proven to be enough to properly characterise the influence of an ionic current on the analysed properties.

### 2.2. Fiber and tissue simulations

Uni-dimensional (1D) fibers of 1 cm length are used to simulate electrical propagation and measure conduction velocity (CV). The fiber is stimulated by a twice diastolic threshold current of 2 ms duration applied at one of its ends at a CL=1000 ms for 5 min. CV is obtained at steady-state by computing the ratio between the distance separating two distant nodes and the time taken by the last wavefront to propagate between them.

In bi-dimensional (2D) tissue simulations, two sizes are used:  $1 \times 1 \text{ cm}^2$  for calculation of the effective refractory period (ERP) and  $5 \times 5 \text{ cm}^2$  for re-entry characterisation. In the  $1 \times 1 \text{ cm}^2$  mesh, stimuli of twice diastolic threshold amplitude and 2 ms duration are applied at the center of the tissue at  $CL=1000 \text{ ms}$  for 5 min in order to reach steady-state. Then, an extra-stimulus (S2) is applied at the same location for varying coupling interval (CI) with a precision of 1 ms. ERP is defined as the shortest CI that ensures propagation following S2.

In the  $5 \times 5 \text{ cm}^2$  mesh, re-entrant activity is initiated by applying a cross-field stimulation protocol. A planar wavefront is initiated at the lower tissue edge, followed by an S2 stimulus applied on a square area in the tissue left-lower corner at a CI within the vulnerable window. The duration of simulations is 10 s. The corresponding pseudo-electrocardiogram (pseudo-ECG) for each re-entry simulation is calculated as in a previous study [3]. The dominant frequency (DF) is obtained after the 10-s stimulation from the pseudo-ECG power spectral density in a window of 2 s width with a precision of 0.1 Hz.

### 2.3. Computational tools

Single cell simulations are conducted using C++ code and the forward Euler method with a time step of 0.02 ms. The open source finite-element software package Chaste ([www.comlab.ox.ac.uk/chaste](http://www.comlab.ox.ac.uk/chaste)) is used to conduct the fibre and tissue simulations on grid computing facilities through the use of the middleware platform Nimrod/G [4]. A mesh resolution of  $250 \mu\text{m}$ , fine enough to make ERP and CV values converge, and time steps of 0.005 and 0.01 ms are used to solve ordinary and partial differential equations, respectively, in the monodomain equation. The diffusion coefficient is set to  $1.3 \text{ cm}^2/\text{s}$ .

## 3. Results

### 3.1. Cell properties

As shown in Figure 1, significant changes in steady-state APD and  $V_{rest}$  values following alterations in certain ionic current conductances can be observed, both in control and following AFER. Particularly, alterations in  $G_{K1}$  and  $G_{NaK}$  entail the largest AP modifications.  $G_{K1}$  inhibition results in significant APD prolongation (and repolarization failure for larger degrees of inhibition, not shown) as well as  $V_{rest}$  depolarization, as it is expected from a decrease in a potassium outward current and consistent with experimental studies [5]. When  $G_{K1}$  is over-expressed, APD is notably shortened and  $V_{rest}$  is lowered (Figure 1). Regarding  $G_{NaK}$ , its inhibition results in APD shortening and  $V_{rest}$  hyperpolarization in control but el-

evation in AFER, as it occurs under ischemic conditions [6], whereas its upregulation leads to APD lengthening and slight changes in  $V_{rest}$  in control but notable elevation in AFER. The rest of the conductances do not have very significant effects on steady-state AP as compared to  $G_{K1}$  and  $G_{NaK}$ .

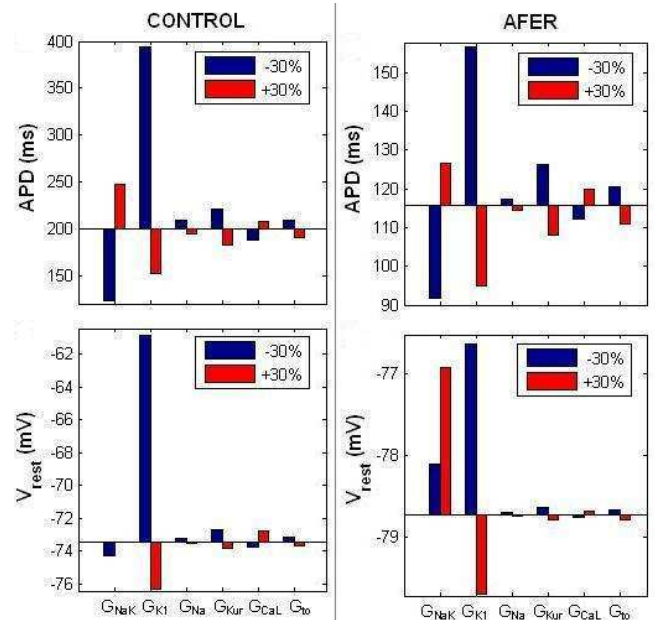


Figure 1. Control (left) vs. AFER (right) APD and  $V_{rest}$  in steady-state after  $\pm 30\%$  conductances alterations.

Interesting differences between control and AFER are observed in the modulation of steady-state AP properties. Figure 1 shows smaller scales in AFER than control, indicating smaller induced changes. The relative relevance of conductances other than  $G_{K1}$  and  $G_{NaK}$  on AP, such as  $G_{Kur}$ ,  $G_{CaL}$  and  $G_{to}$ , is enhanced in AFER conditions, although is still notably smaller than that of  $G_{K1}$  and  $G_{NaK}$  (Figure 1). It is remarkable that inhibition of  $G_{NaK}$  implies opposite changes in  $V_{rest}$  in control (hyperpolarization) and AFER (depolarization). Regarding  $G_{NaK}$  upregulation, it leads to insignificant changes in  $V_{rest}$  in control, whereas  $V_{rest}$  is significantly depolarized when upregulation is simulated in AFER.

In Tables 1 (control) and 2 (AFER) the steady-state values of APD and  $V_{rest}$  after blocking  $G_{K1}$ ,  $G_{NaK}$  and  $G_{Na}$  by 30% are shown. Figure 2 shows steady-state APs when  $G_{K1}$ ,  $G_{NaK}$  and  $G_{Na}$  are respectively altered in a range between -100% and +100% from their default values.

### 3.2. Tissue properties

In tissue, ERP is found to be highly sensitive to alterations in  $G_{NaK}$  and  $G_{K1}$  as well, with more notable changes in control than AFER. That sensitivity can be ex-

Table 1. Steady-state values after 30% blocks in control.

|                 | Default | $\downarrow G_{NaK}$ | $\downarrow G_{K1}$ | $\downarrow G_{Na}$ |
|-----------------|---------|----------------------|---------------------|---------------------|
| APD (ms)        | 200     | 122.8                | 394.6               | 209.8               |
| $V_{rest}$ (mV) | -73.44  | -74.26               | -60.87              | -73.27              |
| ERP (ms)        | 217     | 161                  | *                   | 260                 |
| CV (cm/s)       | 47.97   | 44.44                | *                   | 37.12               |

\*Repolarization failure

Table 2. Steady-state values after 30% blocks in AFER.

|                 | Default | $\downarrow G_{NaK}$ | $\downarrow G_{K1}$ | $\downarrow G_{Na}$ |
|-----------------|---------|----------------------|---------------------|---------------------|
| APD (ms)        | 200     | 91.6                 | 156.6               | 117.2               |
| $V_{rest}$ (mV) | -78.72  | -78.11               | -76.64              | -78.69              |
| ERP (ms)        | 217     | 129                  | 179                 | 193                 |
| CV (cm/s)       | 46.17   | 48.69                | 48.19               | 34.51               |

plained by the dependency of APD and  $V_{rest}$  on those conductances. Block of  $G_{NaK}$  by 30% entails shortening of steady-state ERP whereas its upregulation leads to ERP lengthening. Block of  $G_{K1}$  implies ERP lengthening and, after 4 minutes, cells fail to repolarize becoming unexcitable. This phenomenon is not observed in single cells.  $G_{K1}$  overexpression implies ERP shortening, as expected. Furthermore, apart from  $G_{K1}$  and  $G_{NaK}$ ,  $G_{Na}$  also plays an important role in determining ERP, prolonging it when blocked and shortening it when overexpressed. An important difference is found when comparing control and AFER.  $G_{K1}$  and  $G_{NaK}$  are the most important modulators of ERP in control but the relative importance of  $G_{Na}$  on ERP is enhanced in AFER.

Regarding CV,  $G_{Na}$  is proven to be key in its determination due to its close relationship with cellular excitability. Inhibition of  $G_{Na}$  slows CV, whereas its overexpression accelerates propagation. In addition to  $G_{Na}$ , only  $G_{K1}$  block leads to significant changes in CV due to the strong depolarization of  $V_{rest}$ , which causes repolarization failure after 4 minutes, as described above. The influence of the rest of ionic conductances on CV is insignificant.

Steady-state values of ERP and CV after 30% block of  $G_{NaK}$ ,  $G_{K1}$  and  $G_{Na}$  are summarized in Tables 1 (control) and 2 (AFER).

### 3.3. Re-entrant activity

The implications that the mechanisms unraveled in previous sections have in rotor dynamics are investigated in an attempt to shed light into the ionic basis of AF modulation. As expected from our results on cell and tissue properties,  $G_{K1}$ ,  $G_{NaK}$  and  $G_{Na}$  alterations are the interventions exerting the strongest influence in rotor dynamics. It is important to remark that, once established, the re-entrant circuit remains stable for the duration of the simulation in both control and AFER conditions, as opposed to rotor in-

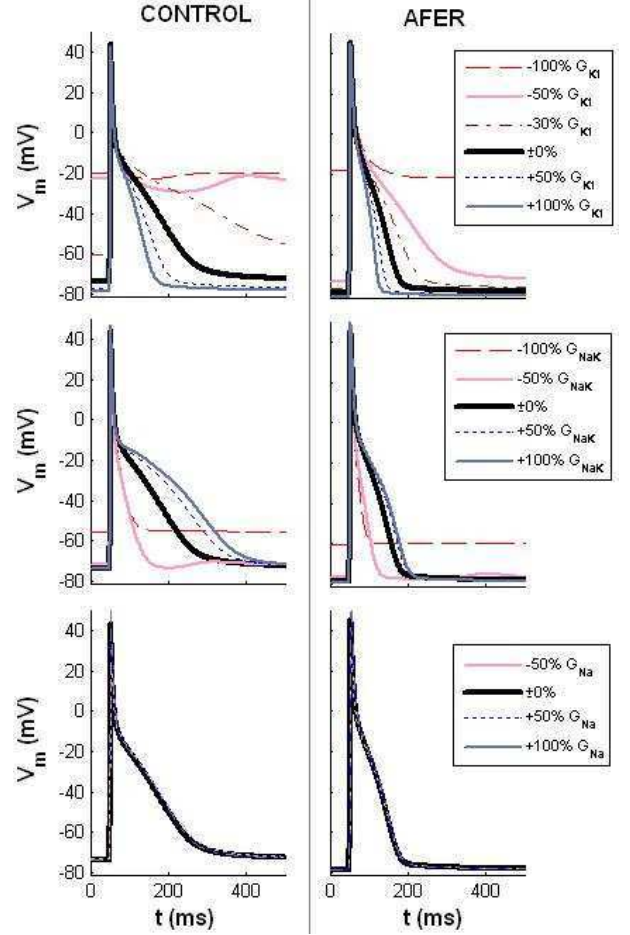


Figure 2. Steady-state AP when  $G_{K1}$ ,  $G_{NaK}$  and  $G_{Na}$  are modified at different levels between -100% and +100% from control (left) and AFER (right).

stability observed with other human atrial tissue models [7]. Figure 3 shows DF of re-entrant rotors calculated after 10-s stimulation for alterations in  $G_{NaK}$ ,  $G_{K1}$  and  $G_{Na}$  in control (blue bars) and AFER (red bars).

Block of either  $G_{NaK}$ ,  $G_{K1}$  or  $G_{Na}$  leads to lower DF values in both control and AFER. The most significant changes occur when  $G_{K1}$  is blocked in control, leading to values of DF below 2 Hz, or when  $G_{Na}$  is blocked in AFER, almost halving the DF value found for unaltered conditions (Figure 3). Not many qualitative differences can be found between control and AFER, but quantitatively DF in AFER reaches values that are 2-3 Hz higher than in control, consistent with previous studies [2].

## 4. Discussion and conclusions

Our study unravels the relative importance of ionic currents in modulating electrophysiological properties, re-entry susceptibility and rotor dynamics in human atrial

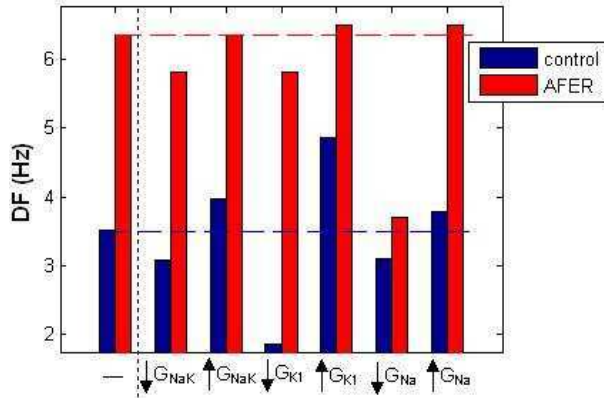


Figure 3. DF values after  $\pm 30\%$  changes in  $G_{NaK}$ ,  $G_{K1}$ ,  $G_{Na}$  in control (blue bars) and AFER (red bars).

tissue in the presence and absence of AFER. We demonstrate that  $G_{NaK}$  is as important as  $G_{K1}$  and  $G_{Na}$  in determining human atrial electrophysiology and rotor dynamics in control and AFER. Results show that the ionic mechanisms determining atrial electrophysiology are qualitatively similar in control and AFER, although quantitative differences can be found.

$I_{K1}$  has been previously highlighted as a very important mechanism in human atrial electrophysiology and its block has been reported to successfully stop arrhythmias in different animal species [8]. This is consistent with the results of our study which show that  $I_{K1}$  block importantly lengthens both APD and ERP.

In this study, the  $Na^+/K^+$  pump has been proven to be essential in modulating cardiac electrophysiological properties. The steady-state APD, and thus ERP, shortening caused by  $G_{NaK}$  inhibition can seem counterintuitive because the inhibition of the pump outward current would be expected to prolong APD. However, additional mechanisms involving an increase in the intracellular sodium and systolic calcium concentrations underlie the observed APD shortening, in good agreement with experimental studies showing that strong blockade of  $Na^+/K^+$  pump using strophantidin leads to an initial APD lengthening followed by a progressive shortening [9].

Sodium channel blockers, targeting  $I_{Na}$ , are widely used for short term AF treatment due to its clear influence on ERP and CV, in accordance with the observations of this study [2]. However, there is much controversy in the use of Class I drugs due to their potential pro-arrhythmic effects on the ventricles. Identification of atrial-selective drugs is a promising approach to treat AF.

In this study, a systematic analysis is conducted to quantify the role of ionic current conductances in modulating atrial electrophysiological properties before and after AFER. Simulations confirm  $G_{NaK}$ ,  $G_{K1}$  and  $G_{Na}$  as key

contributors to AF-related electrophysiological properties in human atria. Overall, similar results are obtained before and after AFER but with smaller effects on the latter. The in-depth characterization of the ionic basis of atrial electrophysiology and AF-related mechanisms provided here could guide in the identification of more effective therapies against AF.

## Acknowledgements

This study was financially supported by the European Commission preDiCT Grant DG-INFSO-224381 (to B.R.), Royal Society Visiting Fellowship and International Joint Project (to E.P. and B.R.), grants TEC-2011-19140 from Ministerio de Ciencia e Innovacion, Spain and PI 144/2009 from Gobierno de Aragon, Spain (to E.P. and C.S.), and fellowship BES-2008-002522 from Ministerio de Ciencia e Innovacion, Spain (to C.S.); and technically possible thanks to Blair Bethwaite and the Nimrod developers team.

## References

- [1] Maleckar MM, Greenstein JL, Giles WR, Trayanova NA:  $K^+$  current changes account for the rate dependence of the action potential in the human atrial myocyte. *Am J Physiol Heart Circ Physiol* 2009;297:H1398-H1410.
- [2] Pandit SV, Berenfeld O, Anumonwo JMB, Zaritski RM, Kneller J, Nattel S, Jalife J: Ionic determinants of functional reentry in a 2-D model of human atrial cells during simulated chronic atrial fibrillation. *Biophys J* 2005;88:3806-3821.
- [3] Baher A, Qu Z, Hayatdavoudi A, Lamp ST, Yang MJ, Xie F, Turner S, Garfinkel A, Weiss JN: Short-term cardiac memory and mother rotor fibrillation. *Am J Physiol Heart Circ Physiol* 2007;292:H180-H189.
- [4] Abramson D, Bernabeu MO, Bethwaite B, Burrage K, Pueyo E, Rodríguez B, Sher A, Tan K: High-throughput cardiac science on the grid. *Phil Trans R Soc A* 2010;368:3907-3923.
- [5] Dobrev D, Graf E, Wettwer E, Himmel HM, Hála O, Doerfel C, Christ T, Schuler S, Ravens U: Molecular basis of downregulation of G-protein-coupled inward rectifying  $K^+$  current ( $IK_{ACh}$ ) in chronic human atrial fibrillation: decrease in GIRK4 mRNA correlates with reduced  $IK_{ACh}$  and muscarinic receptor-mediated shortening of action potentials. *Circulation* 2001;104:2551-2557.
- [6] Rodríguez B, Ferrero Jr. JM, Trénor B: Mechanistic investigation of extracellular  $K^+$  accumulation during acute myocardial ischemia: a simulation study. *Am J Physiol Heart Circ Physiol* 2002;283:H490-H500.
- [7] Cherry EM, Evans SJ: Properties of two human atrial cell models in tissue: restitution, memory, propagation and reentry. *J Theor Biol* 2008;254:674-690.
- [8] Sato R, Koumi SI, Hisatome I, Takai H, Aida Y, Oyaizu M, Karasaki S, Mashiba H, Katori R: A new class III antiarrhythmic drug, MS-551, blocks the inward rectifier potassium channel in isolated guinea pig ventricular myocytes. *J Pharmacol Exp Ther* 1995;274:469-474.
- [9] Levi A: The effect of strophantidin on action potential, calcium current and contraction in isolated guinea-pig ventricular myocytes. *J Physiol* 1991;443:1-23.

Address for correspondence:

Carlos Sánchez, cstapia@unizar.es,  
DIEC / CPS / University of Zaragoza / Spain